COBEM 2023 27TH INTERNATIONAL CONGRESS OF MECHANICAL ENGENEERING
ABCM Brazilian Society of Mechanical Sciences and Engineering
27th ABCM International Congress of Mechanical Engineering
December 04-08, 2023, Florianópolis-SC, Brazil

COB-2023-0527 TOPOLOGICAL DERIVATIVE IN OPTIMIZATION OF ARCH DAMS

L. Duarte
M. Xavier
Universidade Federal Fluminense - Rua Passo da Pátria, 152-470 - São Domingos, Niterói - RJ, 24210-240
lucasvmad@id.uff.br and marcelxavier@id.uff.br

Abstract. *The design of dams has been the subject of various studies for centuries. Relevant advances in this area have been achieved in recent decades with the support of computational tools. Recently proposed, the topological derivative method has been recognized as a powerful tool due to its successful application in various branches of physics and engineering. Topics such as inverse problems, optimization of structures and mechanical modeling of fracture evolution are cases in which this concept has been used. The topological derivative quantifies the sensitivity of a given shape functional to the nucleation of a disturbance in the domain, such as the insertion of holes, inclusions and even fractures. In this work, this method will be used specifically to optimize structures subject to hydrostatic pressure, with a focus on the design of the horizontal section of arch dams. The computational algorithm, which is based on the topological derivative concept and the level-set domain representation method in the context of plane elasticity, is used to solve the optimization problem. The numerical result obtained by this algorithm is capable of generating an arc-shaped geometry that resembles the horizontal sections characteristic of this type of dam. Therefore, the results of this work suggest that the Topological Derivative Method can be used to develop an algorithm to support the specific context of arch dam projects.*

Keywords: *Topology Optimization, Topological Derivative, Arch-Dams.*

1. INTRODUCTION

The consumption of water resources is a key factor in the socio-economic development of all countries. In this context, large dams play a central role in storing water and generating energy resources. According to the *International Commission On Large Dams* (ICOLD), a large dam is one whose distance from the base to the crest is equal to or greater than 15 meters. The classification mentioned above also applies if this distance decreases to a range of 5 to 15 meters, as long as the dam is capable of retaining more than 3 million cubic meters of fluid. There are several types of large dams. Among the best known are the famous gravity dams (which receive this classification due to the great thickness of the base in relation to the crest) which can be straight or curved along the width of the reservoir Thomas (1976). A notable example of this type of dam is the Hoover Dam, located on the Colorado River in the United States.

Evidently, the safety and performance of a dam can be analyzed based on the stresses and deformations observed in the structure.As reported by (Gruner, 1967), thirty percent of the failures or unsatisfactory performance of a dam are associated with the type of structure and construction, including inadequate design. The role of dam engineers has changed a lot in recent decades. Thanks to the growth of scientific contributions and, consequently, the emergence of new technologies, the surveillance, monitoring, design and analysis tasks involved in this process have improved significantly (Ardebili *et al.*, 2020). For works that use domain representation by *level-set* function in the topological optimization of structures subjected to hydrostatic pressure, see (Picelli *et al.*, 2019) and (Emmendoerfer, 2018). See also (Lu and Tong, 2021), which uses the MIST method (*moving iso-surface threshold*) in each iteration to define and update the topology without directly involving sensitivity analysis. In the specific case of arch dams, see also (Akbari *et al.*, 2011) where a methodology based on *Hermit Splines*, finite element shape sensitivity analysis and taking into account design-dependent loads, is proposed to determine the optimal shape of arch dams.

As originally proposed in Xavier and Novotny (2017), the Topological Derivative Method emerges as a natural tool for dealing with the topological optimization of structures subject to hydrostatic pressure. The Topological Derivative was rigorously introduced by Sokołowski and Żochowski (1999). Since then, it has become a powerful tool with applications in many areas of physics and engineering, including shape and topological optimization, inverse problems, image processing, *design* of microstructures, among others.For a complete breakdown of the Topological Derivative Method and its applications, see the books by Novotny and Sokołowski (2013) and Novotny and Sokołowski (2020), for example. The work presented by Xavier and Novotny (2017) proposes a powerful tool, based on the topological derivative with respect to the nucleation of an inclusion with an inhomogeneous transmission condition, to optimize structures that are partially subjected to the action of hydrostatic pressure. Well-known examples in the literature have been successfully reproduced using the proposed methodology. However, despite the robustness and flexibility of the proposed algorithm, no treatment aimed at optimizing dams is mentioned.

Therefore, in this study, the Topological Derivative Method is applied to propose a topological optimization approach in order to find the optimal shape of the horizontal section of a large arch dam. First, the problem of finding the optimal shape of a horizontal section of an arch dam is written in the form of a minimization problem. Next, the calculation of the sensitivity associated with the nucleation of a circular inclusion that has an non-homogeneous transmission condition at its boundary is presented. From a physical point of view, hydrostatic pressure acts at the interface of the topological perturbation, providing a natural mechanism for dealing with the topological optimization of structures subjected to hydrostatic pressure. Finally, the resulting topological derivative field is used to guide this topological optimization algorithm.

The work is structured as follows. The mechanical problem is presented in the form of an optimization problem in Section 2. Section 3presents the concept and the topological derivative result to the problem in question. In Section 4. , the numerical results of three cases generated by the algorithm are shown. Final remarks and a conclusion are made in Section 5.

2. PROBLEM STATEMENT

In order to formulate the problem of finding the optimal shape of the horizontal section of an arch dam, consider a domain $\mathcal{D} \subset \mathbb{R}^2$, composed of two subdomains, $\Omega := \mathcal{D} \setminus \bar{\omega}$ and ω, where Ω represents the elastic material and ω represents the compliant material that is pressurized, see Figure1.

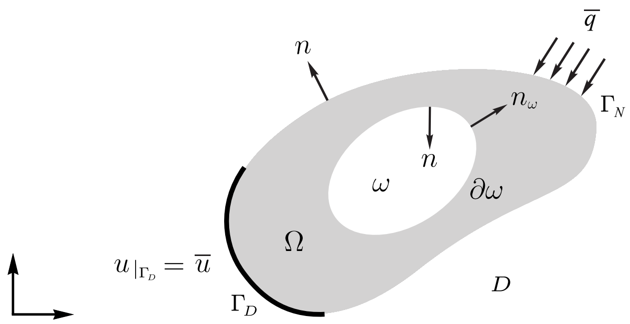

Figure 1. Unperturbed Problem

This mechanical problem can be written as a minimization one as follows:

$$\begin{aligned} &\underset{\Omega \subset \mathcal{D}}{\text{Minimize}} \ -\mathscr{J}_\chi(u) \\ &\text{Subjected to } |\Omega| \leq M, \end{aligned} \tag{1}$$

where M is the amount of material required at the end of the optimization process and $\mathscr{J}_\chi(u)$, given by

$$\mathscr{J}_\chi(u) = \frac{1}{2}\int_{\mathcal{D}} \sigma(u) \cdot (\nabla u)^s - \int_{\Gamma_N} \bar{q} \cdot u - \int_\omega p \operatorname{div} u\,, \tag{2}$$

In order to characterize the elastic and compliant regions, a parameter ρ, defined by

$$\rho = \rho(x) := \begin{cases} 1 & \text{se } x \in \Omega\,, \\ \rho_0 & \text{se } x \in \omega\,, \end{cases} \tag{3}$$

with $\rho_0 \ll 1$, is introduced. This parameter is dimensionless in order to change the elasticity tensor for each material. The term $\sigma(u)$ is the second-order Cauchy stress tensor defined as shown below:

$$\sigma(u) = \rho\mathbb{C}(\nabla u)^s\,, \tag{4}$$

where $\mathbb{C}$ is the fourth-order elasticity tensor given by

$$\mathbb{C} = 2\mu\mathbb{I} + \lambda \mathrm{I} \otimes \mathrm{I}\,. \tag{5}$$

As the domain of analysis corresponds to a horizontal section of the dam, the plane state of stress is considered. The Lamé coefficients μ and λ are constant throughout the domain and are given by:

$$\lambda = \frac{\nu E}{1-\nu^2} \ \text{ and } \ \mu = \frac{E}{2(1+\nu)}\,, \tag{6}$$

for the plane stress state, where E is the modulus of elasticity and ν is the Poisson's ratio. The term $(\nabla u)^s$ is the strain tensor of second order and it's defined as

$$(\nabla u)^s = \frac{1}{2}(\nabla u + (\nabla u)^T)\,, \tag{7}$$

where $u = u(x)$ is the displacement field, which represents the mechanical equilibrium of the system. Finally, $\bar{q}$ is the traction applied on Γ_N and p is the hydrostatic pressure. The linear penalty approach is used to control the volume of material at the end of the optimization process. Other volume control methods can be seen in (Campeão *et al.*, 2014). Thus, the minimization problem is rewritten as:

$$\underset{\Omega \subset \mathcal{D}}{\text{Minimize}}\, F_{\mathcal{X}}(u) = -\mathscr{J}_{\mathcal{X}}(u) + m|\Omega|. \tag{8}$$

where m represents the associated penalty. The shape functional associated to this problem is given by:

$$F_{\mathcal{X}}(u) = \frac{1}{2}\int_{\mathcal{D}} \sigma(u)\cdot(\nabla u)^s - \int_{\Gamma_N} \bar{q}\cdot u - \int_{\omega} p \operatorname{div} u + m\int_{\Omega} 1\,. \tag{9}$$

Then, its weak formulation of the mechanical equilibrium can be written as:

$$\left\{\begin{array}{l} \text{Find}\, u \in \mathscr{U} \text{ such that:} \\ \displaystyle\int_{\mathcal{D}} \sigma(u)\cdot(\nabla\eta)^s = \int_{\Gamma_N} \bar{q}\cdot\eta + \int_{\omega} p \operatorname{div}\eta\,,\ \forall\, \eta \in \mathscr{V}\,, \end{array}\right. \tag{10}$$

with the set $\mathscr{U}$ and $\mathscr{V}$ defined as:

$$\mathscr{U} = \left\{\phi \in H^1(\mathcal{D};\mathbb{R}^2) : [\![\phi]\!]\,|_{\partial\omega} = 0\,,\ \phi\,|_{\Gamma_D} = \bar{u}\right\} \tag{11}$$

$$\mathscr{V} = \left\{\phi \in H^1(\mathcal{D};\mathbb{R}^2) : [\![\phi]\!]\,|_{\partial\omega} = 0\,,\ \phi\,|_{\Gamma_D} = 0\right\}, \tag{12}$$

where $\bar{u}$ is the prescribed displacement on Γ_D and $[\![\phi]\!]$ is the jump.

Also, the strong formulation associated to this problem is written as

$$\left\{\begin{array}{rcll} \multicolumn{4}{l}{\text{Find } u \text{ such that:}} \\ \operatorname{div}\sigma(u) &=& 0 & \text{in } \mathcal{D}\,, \\ \sigma(u) &=& \rho\mathbb{C}(\nabla u)^s & \\ u &=& \bar{u} & \text{on } \Gamma_D\,, \\ \sigma(u)\,n &=& \bar{q} & \text{on } \Gamma_N\,, \\ [\![u]\!] &=& 0 & \text{on } \partial\omega\,, \\ [\![\sigma(u)]\!]\,n &=& -pn & \text{on } \partial\omega\,. \end{array}\right. \tag{13}$$

Since the problem involves an optimization process with respect to changing the topology of the domain, the topological derivative comes naturally as an alternative tool for tackling it. Therefore, the next chapter presents this concept and the topological derivative associated to Eq. (8).

3. TOPOLOGICAL SENSITIVITY ANALYSIS

Firstly, we propose an open and limited domain $\mathcal{D} \subset \mathbb{R}^2$. Then, a topological perturbation is applied inside a small region denoted by $B_\varepsilon(\hat{x}) = \hat{x} + \varepsilon B$, where $\hat{x}$ is any point in $\mathcal{D}$, ε is the radius of B_ε and B is a domain fixed in $\mathbb{R}^2$. Figure 2 illustrates the context in which $B_\varepsilon(\hat{x}) \subset \mathcal{D}$.

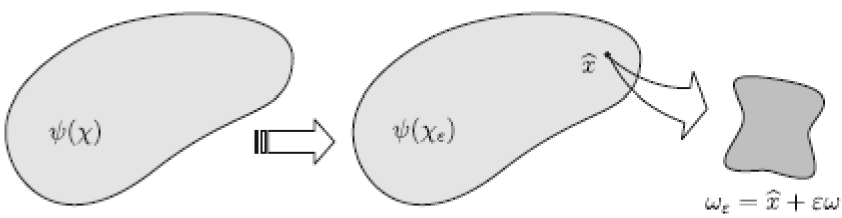

Figure 2. Unperturbed and perturbed domain

A characteristic function $x \mapsto \mathcal{X}(x)$, where $x \in \mathbb{R}^2$, is established and is associated with the unperturbed domain $\mathcal{D}$, so that $\mathcal{X}(x) = \mathbb{1}_{\mathcal{D}}$. The relationship between this characteristic function $\mathcal{X}$ and the unperturbed domain $\mathcal{D}$ is given by the expression:

$$|\mathcal{D}| = \int_{\mathbb{R}^2} \mathcal{X}\,, \tag{14}$$

where $|\mathcal{D}|$ is the Lebesgue measure of $\mathcal{D}$. Then, the characteristic function $x \mapsto \mathcal{X}_\varepsilon(\hat{x})$ is established, which is associated with the topologically perturbed domain $\mathcal{D}_\varepsilon = \mathcal{D} \setminus \bar{B}_\varepsilon(\hat{x})$. After that, it's assumed that the functional of the perturbed problem $\psi(\mathcal{X}_\varepsilon)$ admits an asymptotic expansion as follows:

$$\psi(\mathcal{X}_\varepsilon) = \psi(\mathcal{X}) + D_T\psi(\hat{x})f(\varepsilon) + \mathscr{R}(\varepsilon)\,, \tag{15}$$

where $\psi(\mathcal{X}_\varepsilon)$ is the functional associated with the perturbed problem, $\psi(\mathcal{X})$ is the functional associated with the unperturbed problem, $D_T\psi(\hat{x})$ is the topological derivative of ψ in $\hat{x}$, $f(\varepsilon)$ is the first-order correction function and $\mathscr{R}(\varepsilon)$ is the residual term. The Topological Derivative term is defined as the function $\hat{x} \mapsto D_T\psi(\hat{x})$ of ψ on $\hat{x}$. Reorganizing and taking the limit when $\varepsilon \to 0$ in (15) gives us:

$$D_T\psi(\hat{x}) = \lim_{\varepsilon \to 0} \frac{\psi(\mathcal{X}_\varepsilon) - \psi(\mathcal{X})}{f(\varepsilon)} + \lim_{\varepsilon \to 0} \frac{\mathscr{R}(\varepsilon)}{f(\varepsilon)}\,. \tag{16}$$

Assuming by hypothesis that the quotient $\mathscr{R}(\varepsilon)/f(\varepsilon)$ is a $o(f(\varepsilon))$, that is, it tends to zero when $\varepsilon \to 0$, (16) is finally expressed according to the definition of Topological Derivative of Sokołowski and Żochowski (1999):

$$D_T\psi(\hat{x}) = \lim_{\varepsilon \to 0} \frac{\psi(\mathcal{X}_\varepsilon) - \psi(\mathcal{X})}{f(\varepsilon)}\,. \tag{17}$$

3.1 Perturbed Problem

As shown in Section 3, the first step in calculating the topological derivative is to perturb the problem. The perturbed problem is obtained by nucleating a small pressurized circular inclusion $B_\varepsilon(\hat{x})$ in the domain as in Fig. (3).

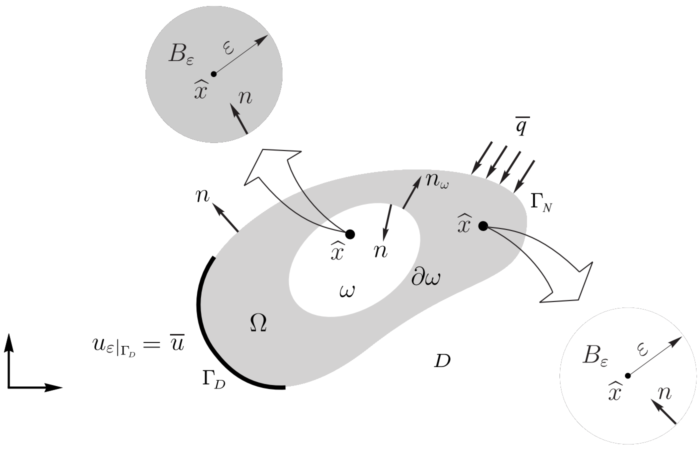

Figure 3. Perturbed Problem

The shape functional associated with the perturbed problem is then given by:

$$F_{\mathcal{X}_\varepsilon}(u_\varepsilon) = \frac{1}{2}\int_{\mathcal{D}} \sigma_\varepsilon(u_\varepsilon)\cdot(\nabla u_\varepsilon)^s - \int_{\Gamma_N} \bar{q}\cdot u_\varepsilon - \int_\omega p\,\mathrm{div}\,u_\varepsilon - \kappa\int_{B_\varepsilon} p\,\mathrm{div}\,u_\varepsilon + m\int_{\Omega_\varepsilon} 1\,, \tag{18}$$

where the Cauchy stress tensor in this case is defined by

$$\sigma_\varepsilon(u_\varepsilon) = \gamma_\varepsilon\sigma(u_\varepsilon)\,, \tag{19}$$

with parameter γ_ε, used to characterize the inclusion, defined as follows:

$$\gamma_\varepsilon = \gamma_\varepsilon(x) := \begin{cases} 1 & \text{se } x \in \mathcal{D}\setminus\bar{B}_\varepsilon\,, \\ \gamma & \text{se } x \in B_\varepsilon\,. \end{cases} \tag{20}$$

The γ parameter represents the contrast in the material property which is defined by

$$\gamma = \gamma(x) := \begin{cases} \rho_0 & \text{se } x \in \Omega\,, \\ \rho_0^{-1} & \text{se } x \in \omega\,, \end{cases} \tag{21}$$

which induces the domain representation method by level-set function. The parameter κ is introduced to control where the topological perturbation B_ε is nucleated, either in Ω or in ω, and is defined as

$$\kappa = \kappa(x) := \begin{cases} +1 & \text{se } x \in \Omega\,, \\ -1 & \text{se } x \in \omega\,. \end{cases} \tag{22}$$

The weak formulation of this case is presented below

$$\begin{cases} \text{Find } u_\varepsilon \in \mathscr{U}_\varepsilon \text{ such that:} \\ \displaystyle\int_{\mathcal{D}} \sigma_\varepsilon(u_\varepsilon) \cdot (\nabla\eta)^s = \int_{\Gamma_N} \bar{q} \cdot \eta + \int_\omega p \operatorname{div} \eta + \kappa \int_{B_\varepsilon} p \operatorname{div} \eta \,, \ \forall\, \eta \in \mathscr{V}_\varepsilon \,, \end{cases} \tag{23}$$

where the set $\mathscr{U}_\varepsilon$ and $\mathscr{V}_\varepsilon$ are defined as

$$\mathscr{U}_\varepsilon = \Big\{ \phi \in H^1(\mathcal{D};\mathbb{R}^2) : [\![\phi]\!] \,|_{\partial B_\varepsilon} = 0 \,, \phi \,|_{\Gamma_D} = \bar{u} \Big\} \tag{24}$$

$$\mathscr{V}_\varepsilon = \Big\{ \phi \in H^1(\mathcal{D};\mathbb{R}^2) \,: [\![\phi]\!] \,|_{\partial B_\varepsilon} = 0 \,, \phi \,|_{\Gamma_D} = 0 \Big\} \,. \tag{25}$$

Its strong formulation is written as follows:

$$\begin{cases} \text{Find } u_\varepsilon \text{ such that:} & & & \\ \operatorname{div}\sigma_\varepsilon(u_\varepsilon) &=& 0 & \text{in } \mathcal{D} \,, \\ \sigma_\varepsilon(u_\varepsilon) &=& \gamma_\varepsilon \, \sigma(u_\varepsilon) & \\ u_\varepsilon &=& \bar{u} & \text{on } \Gamma_D \,, \\ \sigma(u_\varepsilon)\, n &=& \bar{q} & \text{on } \Gamma_N \,, \\ [\![u_\varepsilon]\!] &=& 0 & \text{on } \partial\omega \,, \\ [\![\sigma_\varepsilon(u_\varepsilon)]\!]\, n &=& -pn & \text{on } \partial\omega \,, \\ [\![u_\varepsilon]\!] &=& 0 & \text{on } \partial B_\varepsilon \,, \\ [\![\sigma_\varepsilon(u_\varepsilon)]\!]\, n &=& -\kappa pn & \text{on } \partial B_\varepsilon \,. \end{cases} \tag{26}$$

3.2 Topological Derivative Existence

The existence of the topological derivative for the problem in question is guaranteed by the lemma below

Lema 3.21. *Let u_ε be the solution of the perturbed problem (26) and u the solution of the unperturbed problem (13). Thus, the following estimate is valid:*

$$\|u_\varepsilon - u\|_{H^1(\mathcal{D},\mathbb{R}^2)} \le C\varepsilon \,.$$

Proof. Subtracting (10) from (23) and using the contrast definition Eq. (20) we have

$$\kappa \int_{B_\varepsilon} p \operatorname{div} \eta = \int_{\mathcal{D}} \big[\sigma_\varepsilon(u_\varepsilon) - \sigma(u)\big] \cdot (\nabla\eta)^s \,. \tag{27}$$

Adding and subtracting the term

$$\int_{B_\varepsilon} \gamma\sigma(u) \cdot (\nabla\eta)^s \,, \tag{28}$$

we obtain:

$$\kappa \int_{B_\varepsilon} p \operatorname{div} \eta = \int_{\mathcal{D}} \sigma_\varepsilon(u_\varepsilon - u) \cdot (\nabla\eta)^s + (\gamma - 1) \int_{B_\varepsilon} \sigma(u) \cdot (\nabla\eta)^s \,. \tag{29}$$

Assuming $\eta = u_\varepsilon - u$ in the above expression provides

$$\int_{\mathcal{D}} \sigma_\varepsilon(u_\varepsilon - u) \cdot (\nabla(u_\varepsilon - u))^s + (\gamma - 1) \int_{B_\varepsilon} \sigma(u) \cdot (\nabla(u_\varepsilon - u))^s = \kappa \int_{B_\varepsilon} p \operatorname{div}(u_\varepsilon - u) \,. \tag{30}$$

We put all B_ε integrals together leading to:

$$\int_{\mathcal{D}} \sigma_\varepsilon(u_\varepsilon - u) \cdot (\nabla(u_\varepsilon - u))^s = \int_{B_\varepsilon} T(u) \cdot (\nabla(u_\varepsilon - u))^s \,, \tag{31}$$

where $T(u) = \big[(1-\gamma)\sigma(u) - \kappa pI\big]$. Applying the Cauchy-Schwarz inequality in Eq. (31) we have

$$\begin{aligned} \int_{\mathcal{D}} \sigma_\varepsilon(u_\varepsilon - u) \cdot (\nabla(u_\varepsilon - u))^s &\le \|T(u)\|_{L^2(B_\varepsilon,\mathbb{R}^2)} \, \|(\nabla(u_\varepsilon - u))^s\|_{L^2(B_\varepsilon,\mathbb{R}^2)} \\ &\le c_0\varepsilon \, \|(\nabla(u_\varepsilon - u))^s\|_{L^2(B_\varepsilon,\mathbb{R}^2)} \\ &\le c_1\varepsilon \, \|u_\varepsilon - u\|_{H^1(\mathcal{D},\mathbb{R}^2)} \,. \end{aligned} \tag{32}$$

Using the coercivity of bilinear form on the left side of the above expression leads to

$$c_2\|u_\varepsilon - u\|^2_{H^1(\mathcal{D})} \leq \int_{\mathcal{D}} \sigma_\varepsilon(u_\varepsilon - u)\cdot(\nabla(u_\varepsilon - u))^s \\ \leq c_1\varepsilon\,\|u_\varepsilon - u\|_{H^1(\mathcal{D},\mathbb{R}^2)}\,. \tag{33}$$

As expected, the existence of the topological derivative is guaranteed by the inequality we obtain

$$\|u_\varepsilon - u\|_{H^1(\mathcal{D},\mathbb{R}^2)} \leq C\varepsilon\,. \tag{34}$$

where $C = c_1/c_2$ is a constant independent of ε. □

3.3 Formula of the Topological Derivative

To solve the minimization problem stated in Eq. (8), we need to calculate the topological derivative of the the total potential energy and the volume constraint as following:

$$D_T F_\chi(u) = -D_T\mathscr{J}_\chi(u) + D_T(m|\Omega|)\,. \tag{35}$$

The term $D_T(m|\Omega|)$ is easily obtained and its result is

$$D_T(m|\Omega|) = -\kappa(x)m\,,\ \forall x\in\mathcal{D}\,, \tag{36}$$

where $\kappa(x)$ defined in Eq. (22).As the focus of this article is not the development of the topological derivative of the total potential, the reader is invited to check those steps in (Xavier and Novotny, 2017). Thus, the final expression of $D_T\mathscr{J}_\chi(u)$ is stated as

$$D_T\mathscr{J}_\chi(u) = -\mathbb{P}_\gamma\sigma(u)(\hat{x})\cdot(\nabla u(\hat{x}))^s - \frac{\alpha+1}{1+\alpha\gamma}\kappa p\,\mathrm{div}\,u(\hat{x}) - \frac{p^2}{2\mu\rho(1+\alpha\gamma)}\,, \tag{37}$$

where $\mathbb{P}_\gamma$ is the isotropic polarization tensor of fourth order for a circular inclusion, according to (Ammari and Kang, 2007), and is given by:

$$\mathbb{P}_\gamma = \frac{(1-\gamma)}{2(1+\beta\gamma)}\left[(1+\beta)\mathbb{I} + \frac{(1-\gamma)(\alpha-\beta)}{2(1+\alpha\gamma)}\,\mathrm{I}\otimes\mathrm{I}\right]. \tag{38}$$

The constants α and β are defined as

$$\alpha = \frac{\lambda+\mu}{\mu} \quad\text{and}\quad \beta = \frac{\lambda+3\mu}{\lambda+\mu}\,. \tag{39}$$

We can take the limits when $\gamma\to 0$ and $\gamma\to\infty$ in Eq. (38) because we are using a very compliant material to mimic the water.So, when $\gamma\to 0$, there is a hole with the transmission condition on the inclusion boundary degenerating into a non-homogeneous Neumann boundary condition. The topological derivative for the elastic material in this case is

$$D_T\mathscr{J}_\chi(u) = -\mathbb{P}_0\,\sigma(u)(\hat{x})\cdot(\nabla u(\hat{x}))^s - (\alpha+1)\,p\,\mathrm{div}\,u(\hat{x}) - \frac{p^2}{2\mu}\,,\forall\hat{x}\in\Omega\,, \tag{40}$$

where its polarization tensor $\mathbb{P}_0$ is shown below

$$\mathbb{P}_0 = \frac{1+\beta}{2}\mathbb{I} + \frac{\alpha-\beta}{4}\,\mathrm{I}\otimes\mathrm{I}\,. \tag{41}$$

For $\gamma\to\infty$, there is an elastic inclusion turning into a rigid one. In that case, the topological derivative for the compliant material is

$$D_T\mathscr{J}_\chi(u) = -\mathbb{P}_\infty\,\sigma(u)(\hat{x})\cdot(\nabla u(\hat{x}))^s\,,\forall\hat{x}\in\omega\,, \tag{42}$$

where the polarization tensor $\mathbb{P}_\infty$ is given by

$$\mathbb{P}_\infty = -\frac{1+\beta}{2\beta}\mathbb{I} + \frac{\alpha-\beta}{4\alpha\beta}\,\mathrm{I}\otimes\mathrm{I}\,. \tag{43}$$

4. NUMERICAL EXPERIMENT

To solve the minimization problem in Eq. (8), it's used the algorithm developed by (Amstutz and Andrä, 2006). Their algorithm is based on the topological derivative and the domain representation method by the level-set function. See in (Amstutz, 2011) for more explanations about it. Its application in different problems were presented in (Torii *et al.*, 2016), (Giusti *et al.*, 2017), (Giusti *et al.*, 2019), (Amigo *et al.*, 2016), (Amstutz and Novotny, 2010), (Amstutz *et al.*, 2012) and (Sá *et al.*, 2016). The general parameters used in the example are presented in Tab. 4.

Table 1. Parameters

Parameter	Value
E (GPa)	47
ν	0.21
p (MPa)	1.47
ρ_0	10^{-6}
m	250

The material properties adopted are listed in the concrete report by (ACI Comittee, 1996). The hydrostatic pressure was calculated adopting a height of 150 meters from the surface to its center of gravity.

The topology consists in the elastic material distribution (Ω) and the compliant material (ω), which represents the water. The region ω is pressurized during the whole optimization process. The problem is discretized into linear triangular finite elements. The representation of domain $\mathcal{D}$ of this numerical result is shown in the Fig. (4) and its parameters are listed in Tab. 4.The thicker black line in Fig. (4) represents the clamped boundary condition.

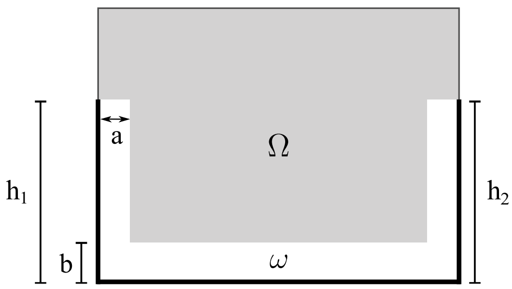

Figure 4. Domain $\mathcal{D}$

Table 2. Parameters of the Domain $\mathcal{D}$

Parameter	Value (km)
h_1	0.2
h_2	0.05
w	0.009

When the algorithm ends the iteration process, it asks for a mesh refinement. So, in order to obtain a better resolution, three uniform mesh refinements were made to provide the final topology in Fig. (5). Notice that this topology is similar to results presented in (Picelli *et al.*, 2019) and (Lu and Tong, 2021).

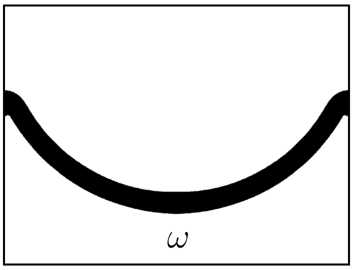

Figure 5. Final Topology

Figure (6) shows the shape functional. The entire procedure consisted of 29 iterations, and at the end of these iterations, the final volume obtained was approximately 10% of the initial volume.

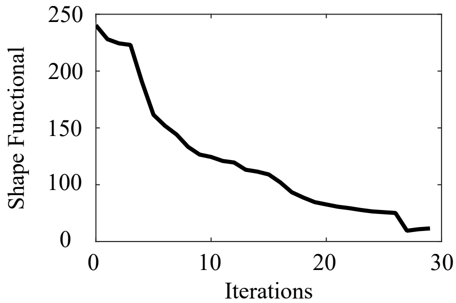

Figure 6. History of the shape functional $F_\chi(u)$ values

The divergent of u in Fig. (7) is plotted and indicates that there is only compressive stress in the arch.

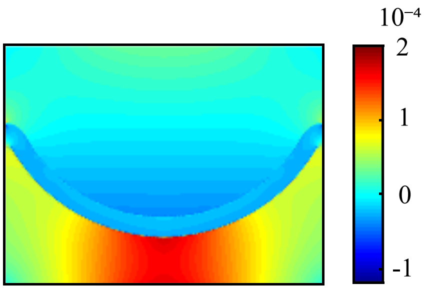

Figure 7. Divergent of u

5. CONCLUSION

In this work, the topological derivative method was used to optimize structures subjected to hydrostatic pressure in the context of arch dams. Initially, the problem of finding the optimum shape of a horizontal section of an arch dam was written in the form of a minimization problem. Then, the entire derivation of the associated topological derivative field was presented. The computational algorithm proposed by (Amstutz and Andrä, 2006), which is based on the topological derivative field and the level-set function domain representation method, was then used in combination with the topological derivative obtained to optimize a structure subjected to hydrostatic pressure with the aim of obtaining arch-shaped topologies. As mentioned, the strategy basically consisted of introducing a lateral load in order to induce the final topology to a local minimum that corroborated with the expected topology. Although this primary objective was achieved, the non-convergence of the θ angle reveals a limitation of the model.

6. ACKNOWLEDGEMENTS

This research was partly supported by CAPES (Brazilian Higher Education Staff Training Agency).

7. REFERENCES

ACI Comittee, 1996. “Aci 207.1r-96: Mass concrete”. Technical report, American Concrete Institute.

Akbari, J., Ahmadi, M. and Moharrami, H., 2011. “Advances in concrete arch dams shape optimization”. *Applied Mathematical Modelling*, Vol. 35, No. 7, pp. 3316–3333.

Amigo, R., Giusti, S., Novotny, A., Silva, E. and Sokolowski, J., 2016. “Optimum design of flextensional piezoelectric actuators into two spatial dimensions”. *SIAM Journal on Control and Optimization*, Vol. 52, No. 2, pp. 760–789. doi:10.1137/151004860.

Ammari, H. and Kang, H., 2007. *Polarization and moment tensors with applications to inverse problems and effective medium theory*. Applied Mathematical Sciences vol. 162. Springer-Verlag, New York.

Amstutz, S., 2011. “Analysis of a level set method for topology optimization”. *Optimization Methods and Software*, Vol. 26, No. 4-5, pp. 555–573.

Amstutz, S. and Andrä, H., 2006. “A new algorithm for topology optimization using a level-set method”. *Journal of Computational Physics*, Vol. 216, No. 2, pp. 573–588.

Amstutz, S. and Novotny, A., 2010. “Topological optimization of structures subject to von Mises stress constraints”. *Structural and Multidisciplinary Optimization*, Vol. 41, No. 3, pp. 407–420.

Amstutz, S., Novotny, A. and de Souza Neto, E., 2012. “Topological derivative-based topology optimization of structures subject to Drucker-Prager stress constraints”. *Computer Methods in Applied Mechanics and Engineering*, Vol. 233–236, pp. 123–136.

Ardebili, M., Salamon, J., Mazza, G., Tosun, H. and Xu, B., 2020. *Advances in Dam Engineering*, Vol. 1. MDPI. ISBN 978-3-03936-327-8.

Campeão, D., Giusti, S. and Novotny, A., 2014. “Topology design of plates consedering different volume control methods”. *Engineering Computations*, Vol. 31, No. 5, pp. 826–842.

Emmendoerfer, H., 2018. “Level set topology optimization for design-dependent pressure load problems”. *International Journal for Numerical Methods in Engineering*, Vol. 115, No. 7, pp. 1–28.

Giusti, S., Mróz, Z., Novotny, A. and Sokołowski, J., 2019. “Topology design of thermomechanical actuators combined with heat source optimization”. *Pure and Applied Functional Analysis*, Vol. 4, No. 4, pp. 825–848.

Giusti, S., Mróz, Z., Sokołowski, J. and Novotny, A., 2017. “Topology design of thermomechanical actuators”. *Structural and Multidisciplinary Optimization*, Vol. 55, pp. 1575–1587.

Gruner, E., 1967. “The mechanism of dam failure”. In 9^{th} *International Congress on Large Dams*. Istanbul, Turkey, Vol. 11, pp. 197–206.

Lu, Y. and Tong, L., 2021. “Topology optimization of compliant mechanisms and structures subjected to design-dependent pressure loadings”. *Structural Multidisciplinary Optimization*, Vol. 63, No. 9, pp. 1889–1906.

Novotny, A. and Sokołowski, J., 2013. *Topological derivatives in shape optimization*. Interaction of Mechanics and Mathematics. Springer-Verlag, Berlin, Heidelberg. doi:10.1007/978-3-642-35245-4.

Novotny, A. and Sokołowski, J., 2020. *An introduction to the topological derivative method*. Springer Briefs in Mathematics. Springer Nature Switzerland. doi:10.1007/978-3-030-36915-6.

Picelli, R., Neofytou, A. and Kim, H.A., 2019. “Topology optimization for design-dependent hydrostatic pressure loading via the level-set method”. *Structural Multidisciplinary Optimization*, Vol. 60, No. 5, pp. 1313–1326.

Sá, L., Amigo, R., Novotny, A. and Silva, E., 2016. “Topological derivatives applied to fluid flow channel design optimization problems”. *Structural and Multidisciplinary Optimization*, Vol. 54, No. 2, pp. 249–264.

Sokołowski, J. and Żochowski, A., 1999. “On the topological derivative in shape optimization”. *SIAM Journal on Control and Optimization*, Vol. 37, No. 4, pp. 1251–1272.

Thomas, H.H., 1976. *The engineering of large dams*, Vol. 1. John Wiley and Sons. ISBN 0-471-01528-8.

Torii, A., Novotny, A. and Santos, R., 2016. “Robust compliance topology optimization based on the topological derivative concept”. *International Journal for Numerical Methods in Engineering*, Vol. 106, No. 11, pp. 889–903.

Xavier, M. and Novotny, A., 2017. “Topological derivative-based topology optimization of structures subject to design-dependent hydrostatic pressure loading”. *Structural and Multidisciplinary Optimization*, Vol. 56, No. 1, pp. 47–57.

8. RESPONSIBILITY NOTICE

The authors are solely responsible for the printed material included in this paper.